JOURNAL OF MATERIALS SCIENCE 32 (1997) 5439–5444

Mechanism of the formation of $M_{23}C_6$ plates around undissolved NbC particles in a stabilized austenitic stainless steel

B. SASMAL
Department of Metallurgical and Materials Engineering, Indian Institute of Technology, Kharagpur-721 302, India

The plate-like morphology of $M_{23}C_6$ carbide precipitated around undissolved NbC particles in a stabilized austenitic stainless steel has been studied by transmission electron microscopy. This precipitation occurred during high temperature ageing of the specimens which had previously been quenched in water from 1550 K. These carbide plates that are characterized by {111}- and {101}-type interfaces have a cube–cube orientation relationship with austenite and lie on {110} austenite planes. Such precipitation was not commonly observed in specimens that were deformed prior to ageing. The possible mechanisms for the nucleation and growth of these precipitates are discussed.

1. Introduction

The addition of a stabilizing element such as Ti or Nb to austenitic stainless steels causes the precipitation of MC type carbides in preference to the chromium-rich $M_{23}C_6$ (M = Cr, Fe) phase during ageing of the solution-treated and water-quenched steels. The MC type carbides are precipitated at austenite grain boundaries and twin boundaries, on dislocations, in association with stacking faults, and as random dot-like precipitates [1–10]. A smaller amount of $M_{23}C_6$ also precipitates at highly preferential sites such as grain boundaries and twin boundaries. The $M_{23}C_6$ nucleated at different sites may grow in size assuming various morphologies [11–19]. The present author has previously reported the precipitation of $M_{23}C_6$ around NbC particles [10, 20], on ageing, which remained undissolved during a high temperature annealing prior to quenching in water. The $M_{23}C_6$ grows around undissolved NbC particles with a thin plate morphology which is distinctly different from the reported plate morphology for $M_{23}C_6$ precipitated at other sites in the austenite matrix [14, 17, 19].

In this paper the mechanisms for the nucleation of $M_{23}C_6$ around undissolved NbC particles and their growth into the characteristic thin plate morphology are discussed.

2. Experimental procedure

A DIN 4981 steel having the chemical composition 0.057C, 16.2Cr, 15.8Ni, 1.12Mn, 0.41Si, 1.84Mo, 0.77Nb, 0.022V, 0.007Ti, 0.006S, 0.005P, 0.007N and 0.0003B, expressed in wt %, was used in this study.

Steel sheets of 240 μm in thickness were cold rolled to a thickness of about 100 μm. Pieces of the rolled sheets were sealed in silica tubes under a partial pressure of argon in order to prevent oxidation. The sealed specimens were solution treated for 45 min at 1550 K and quenched in water. In order to obtain a higher cooling rate the silica tubes were broken under water.

The quenched specimens were resealed in silica tubes under vacuum and aged at 1073 K for periods in the range 1–4000 h. In order to study the effect of deformation on the transformation during ageing one set of quenched specimens (thicker than 100 μm) were deformed to a 40% reduction in thickness by rolling at room temperature prior to the ageing treatment.

The microstructures of the quenched as well as aged specimens were characterized by X-ray diffraction, scanning electron microscopy (SEM), energy dispersive X-ray spectroscopy and transmission electron microscopy (TEM). Specimens for the SEM examination were prepared by electrolytic polishing in a solution of sulphuric and phosphoric acids heated to 60 °C. Thin foils for the TEM studies were prepared by twin-jet electrolytic polishing with a mixture of acetic and perchloric acids, maintained below 16°C. Undissolved carbides were extracted from the quenched specimens by dissolving the austenite electrolytically in a solution containing 30 cc HCl, 270 cc H_2O and 20 g of tartaric acid.

3. Results and discussion

3.1. Microstructure of the quenched specimens

The sheet specimens were markedly distorted and sometimes were considerably bent on quenching in water. The specimens contained an appreciable amount of undissolved particles (Fig. 1). Since these particles were very coarse they did not produce an electron diffraction pattern. An X-ray diffraction analysis

0022–2461

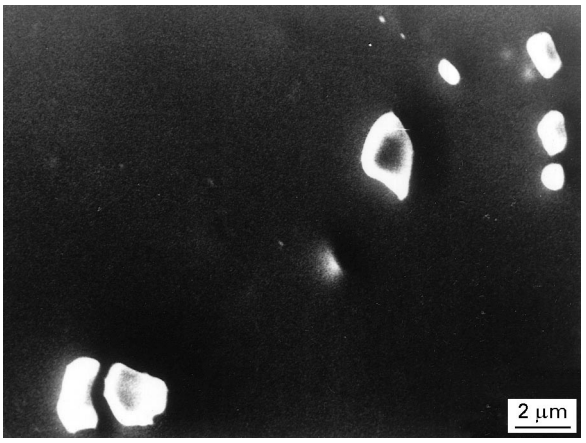

Figure 1 SEM micrograph of a sample water quenched from 1550 K showing undissolved NbC particles.

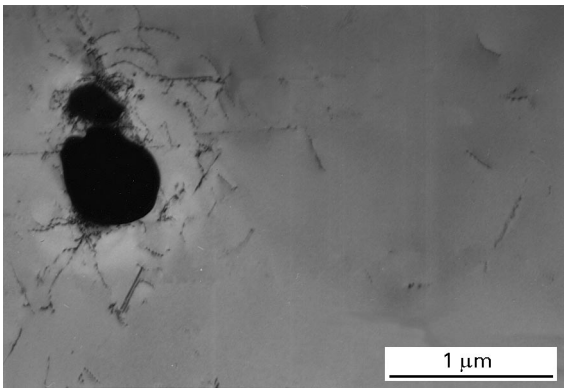

Figure 3 TEM micrograph of a sample water quenched from 1550 K showing a high density of dislocations formed around an undissolved NbC particle.

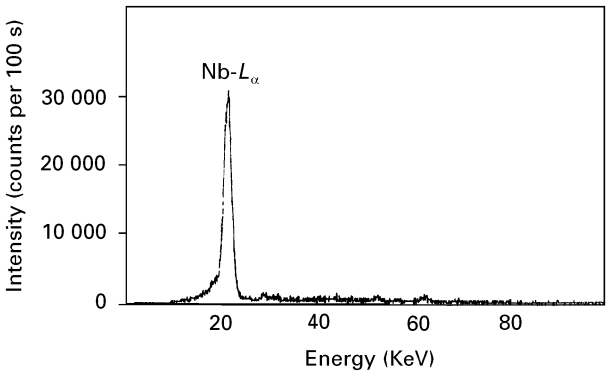

Figure 2 SEM energy dispersive X-ray spectrum of an undissolved NbC particle in the water-quenched specimen.

of the undissolved particles, extracted from the bulk specimens showed that the particles were f.c.c. with a lattice parameter, $a = 0.445$ nm. SEM energy dispersive X-ray spectroscopy showed that these particles contained significant amounts of niobium (Fig. 2). Therefore, these particles are probably a niobium carbide of the type NbC [21]. No other metallic element appeared to be dissolved in these carbide particles. Apart from these undissolved carbides and a few inclusions, the steel was fully austenitic in the quenched state. The lattice parameter of the austenite was 0.359 nm. The density of dislocations was not uniform throughout the austenite grains and was appreciably higher in the vicinity of grain boundaries and around the undissolved particles. The dislocations surrounding the particles were mostly tangled (Fig. 3) although elsewhere they were mostly planar. The specimen foils showed a preferred orientation due to cold rolling – the foil surface being nearly parallel to the {110} planes of austenite.

The specimens deformed by a 40% reduction in thickness after the water quench showed a very high density of dislocations that produced a well developed dislocation cell structure.

3.2. Microstructure of the aged specimens

In the initial stages of ageing, NbC precipitated in a very fine form at the austenite grain boundaries, twin boundaries and on dislocations in the austenite matrix. Gradually the NbC precipitated in association with stacking faults and also as dot-like particles inside the austenite grains. These features of the precipitation are very similar to those reported by other investigators [1–9]. NbC has a cube–cube orientation relationship with the austenite matrix. The $M_{23}C_6$ also precipitated at austenite grain boundaries, twin boundaries and in the austenite matrix, but at a much lower concentration.

On prolonged ageing thin plates were observed that encircled the undissolved NbC particles (Fig. 4). SEM energy dispersive X-ray spectra (Fig. 5 (a–c)) showed that these plates were rich in chromium. Selected area electron diffraction patterns revealed that these precipitates were f.c.c. with a lattice parameter $a = 1.07$ nm, and that they were also cube–cube related to the austenite matrix (Fig. 6). Thus the plates formed around the undissolved NbC particles have been confirmed to be $M_{23}C_6$. Since the coarse undissolved carbides did not produce an electron diffraction pattern, it was not possible to establish whether or not there was an orientation relationship between the undissolved particles and the plates.

The growth rate of the plates of $M_{23}C_6$ is slow. They only acquired equilibrium sizes after nearly 3000 h of ageing at 1073 K, at which point a parallelepiped-shaped plate, as an example, had reached a size of 1.36 and 0.67 μm, with a thickness of 0.07 μm. It was not possible to detect the initial stages of formation of the plates because of the opacity of the undissolved particles to the electron beam. However, after 24 h of ageing, a minor projection was sometimes noted at the surface of some of the particles, and they attained sufficient size to be easily detected after ageing for 100 h. It appears that the $M_{23}C_6$ nucleated at these sites during the early stages of ageing. Analytical studies were possible only after sufficient growth of the plates, i.e. ageing for a very long time.

The morphology and the orientation of a large number of plates were examined by rotating the specimens around the electron beam axis and tilting upto $\pm 45^\circ$ about different axes with the help of a double tilt goniometer stage. By trace analysis it has been found that these plates developed on {110} matrix

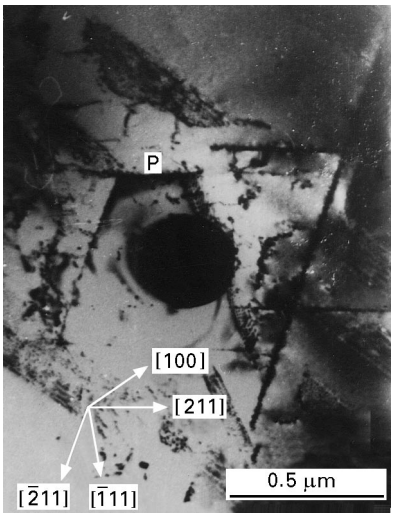

Figure 4 TEM micrograph of a sample aged for 3000 h at 1073 K showing that the $M_{23}C_6$ plate formed around an undissolved NbC particle, at P, lies on (0 1 $\bar{1}$) plane of the matrix. The specimen foil is nearly parallel to (0 1 $\bar{1}$) plane of the matrix. Fine NbC precipitated on dislocations and in association with stacking faults are also present.

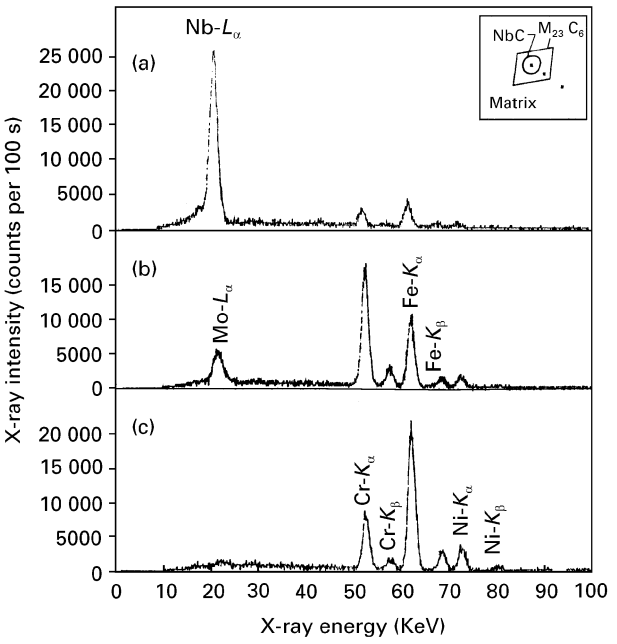

Figure 5 SEM energy dispersive X-ray spectra corresponding to the electron beam placed at different positions: (a) undissolved NbC, (b) a plate around NbC and (c) in the matrix away from the plate. Electron beam positions (x) are shown in a schematic diagram at the top right hand corner.

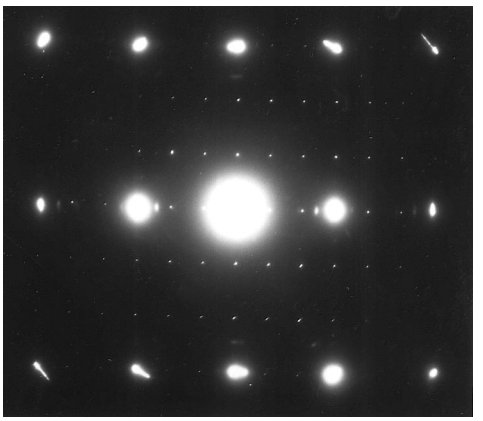

Figure 6 Electron diffraction pattern from an area of the foil having an $M_{23}C_6$ plate formed around an undissolved NbC particle, fine NbC precipitates and the matrix. Matrix, NbC precipitates and the $M_{23}C_6$ plate have the same orientation, (211).

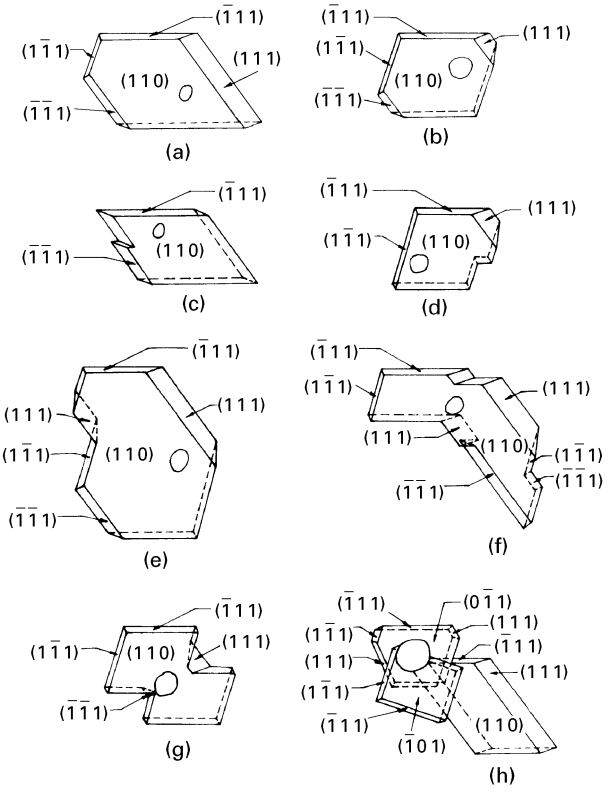

Figure 7 Schematic representation of some observed morphologies of $M_{23}C_6$ plates formed around undissolved NbC particles.

planes and they were limited by {111} planes. One interesting feature is that in most of the cases the plates were observed to lie on the {110} matrix-plane which was nearly parallel to the foil plane. Occasionally, more than one $M_{23}C_6$ plate simultaneously formed around one NbC particle on parallel {110} planes and/or different variants of the {110} planes. The variation in the observed morphology of these plates has been reported elsewhere [10], and a few examples of these are shown schematically in Fig. 7(a–h). In the specimens deformed prior to ageing, the precipitation of $M_{23}C_6$ plates around undissolved NbC particles was not a common feature, although it was occasionally observed.

A hole was often observed to exist in a plate, when it was not attached to an undissolved particle. It is believed that during the course of electrolytic polishing an NbC particle became detached from the specimen leaving a hole in the $M_{23}C_6$ plate. SEM micrographs nearly always showed the presence of NbC particles inside these plates (Fig. 8).

Very often facets were observed at the growing edges of the plates, as is shown in Fig. 7 (a–h) and Moiré fringes were visible at plate–matrix interfaces. This observation suggests that these plates grew by a ledge mechanism [22].

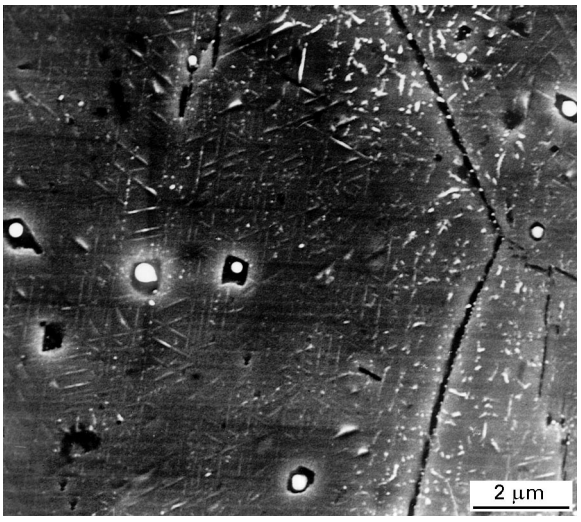

Figure 8 SEM micrograph of a sample aged for 3000 h at 1073 K showing $M_{23}C_6$ precipitated at grain boundaries, twin boundaries and around undissolved NbC particles, and also clusters of fine NbC precipitates.

3.3. Nucleation and growth of $M_{23}C_6$ around undissolved NbC

It is presumed that the $M_{23}C_6$ nucleates at the interface between undissolved NbC particles and the austenite matrix, and then grows into the austenite matrix around these particles. Notable features are that neither does nucleation occur on the entire surface of an undissolved particle nor does a precipitate nucleated at a certain region of the interface, grow to envelope the entire particle surface. The occasional observation of more that one $M_{23}C_6$ plate existing around one NbC particle suggests the presence of several nucleation sites on the particle surface.

The interface between an undissolved particle and the austenite matrix is likely to be incoherent, and can thus provide a nucleation site whose efficiency may be energetically comparable to that of an austenite grain boundary. The expected presence of segregated chromium atoms at the NbC–matrix interface might lead to an early nucleation of $M_{23}C_6$ at these sites. However, the presence of only a limited precipitation at these interfaces indicates that they are comparatively less favourable sites for this nucleation. A competitive precipitation of fine NbC on the dislocations present around an undissolved particle, would account for a reduction in the carbon content in the nearby matrix. This may cause difficulty for the precipitation of $M_{23}C_6$ in these regions. Boundary short circuit diffusion [23] of solutes is also limited because of the small and isolated interfacial areas.

Beckitt and Clark [15] have calculated the atomic configurations of various planes of austenite and $M_{23}C_6$ and have shown that the $\{111\}$ planes of both phases have the highest atomic correspondence, the overall misfit being only 0.99%, with the $\{110\}$ planes also having a close correspondence. $M_{23}C_6$ preferentially nucleates on $\{111\}$ austenite planes because of a minimum energy requirement. At austenite grain boundaries $M_{23}C_6$ does not nucleate continuously but does so at isolated sites [12, 16, 24, 25] and the precipitate distribution is highly sensitive to the degree of grain boundary misorientation. It has been further suggested that the nucleation takes place at a site on the grain boundary where a small group of atoms have a configuration similar to that of a $\{111\}$ plane [12, 16, 26]. At austenite grain boundaries $M_{23}C_6$ nucleates as a thin plate with one surface having a normal high-angle boundary between itself and one austenite grain, and possessing a low-energy interface with the other austenite grain constituting the boundary. The precipitate gradually grows with the migration of the high-angle boundary and becomes embedded in the austenite grain with which it has an orientation relationship and the low energy interface [16, 25].

A similar view may be valid for the nucleation of $M_{23}C_6$ at the interface of an undissolved particle and austenite. It is presumed that $M_{23}C_6$ nucleates at a site on these interfaces where the atomic stacking in austenite is that of $\{111\}$ planes. The precipitate maintains the usual orientation relationship with the austenite grain, as has consistently been observed in this study. Since the size of undissolved particles is very small compared to that of the austenite grains, the curvature of the particle–matrix interfaces is small. This leads to the existence of only a few planar areas along the austenite boundary, at such an interface, that possess the required atomic stacking. This may be one of the reasons for the limited nucleation of $M_{23}C_6$ at these interfaces.

The broad surface of these thin $M_{23}C_6$ plates is always a $\{110\}$ plane whereas the broad surface of $M_{23}C_6$ plates grown elsewhere inside austenite grains is a $\{111\}$ plane [17, 19]. Again the morphologies of $M_{23}C_6$ grown around undissolved NbC particles are different from those of $M_{23}C_6$ grown at other sites [15–17, 19, 25]. It appears that the precipitates of $M_{23}C_6$ which nucleate at the surface of NbC particles grow following a mechanism which is different from those for the precipitation elsewhere.

The interface between an undissolved particle and austenite can not migrate in the manner that a boundary between two austenite grains does during the growth of $M_{23}C_6$ precipitates formed at those sites giving rise to a lath morphology [16, 25]. In the present case, growth of the precipitate along its edge lying at the high energy interface is limited, and instead it grows by the extension of other faces. Since the coherent or semi-coherent interfaces, e.g., $\{111\}$ and $\{110\}$ of $M_{23}C_6$ in the austenite matrix, do not allow rapid atomic transport across them [27, 28], the growth rate of these precipitates in the directions normal to these low energy interfaces is low. Overall growth of these precipitates appears to mainly depend on the availability of solutes at the precipitating sites and also on the formation of ledges along the $\{111\}$ planes of least mismatch.

The observation of a much lower rate of growth along $\langle 110 \rangle$ directions compared to that along $\langle 111 \rangle$ directions which are normal to the planes of least mismatch in an unstrained austenite lattice may be attributed to the modification of strain energy. The strain energy is localized at the precipitation site in the austenite lattice in the presence of a stress field

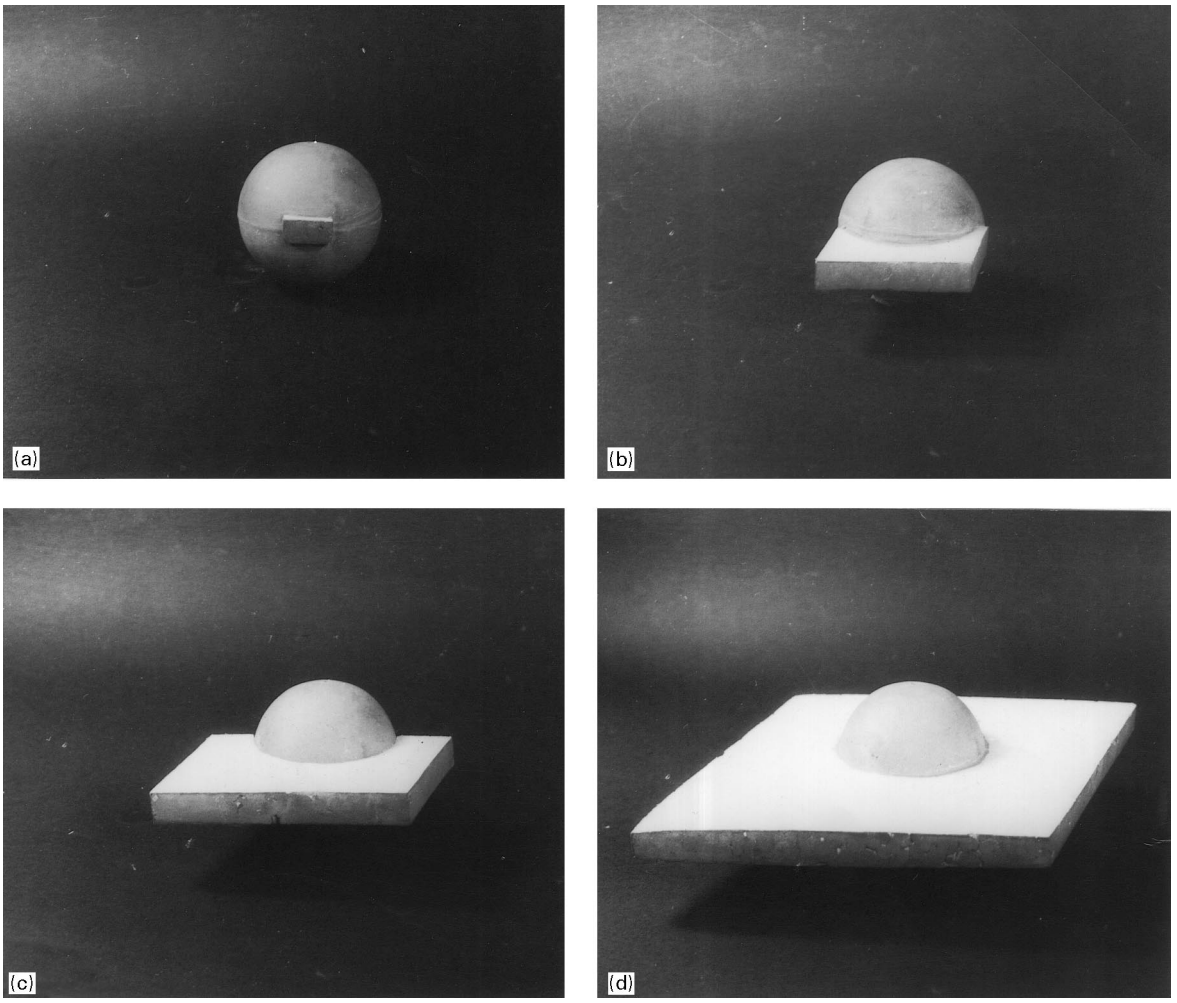

Figure 9 Schematic representation of the nucleation and growth of $M_{23}C_6$ into the characteristic plate morphology developed around an undissolved NbC particle.

produced due to quenching. The presence of a micro-stress in the austenite matrix around the undissolved NbC particles, produced due to the mismatch of thermal contraction between NbC and austenite, seems to influence the precipitate growth leading to the observed morphologies. Further, the occurrence of these $M_{23}C_6$ plates mostly on a $\{110\}$ austenite plane which is nearly parallel to the specimen surface does not find any other explanation except possibly for some influence of the localized residual stress produced due to quenching. During tempering of martensites in steels, an externally applied stress has recently been reported to influence the precipitation of plate-shaped cementite with single crystallographic variants [29, 30].

The broadening and thickening of the $M_{23}C_6$ essentially depends on the formation and migration of ledges at the interface. The migration of planar interfaces is controlled by the lateral movement of ledges at the interphase interface [27, 31, 32]. It is suggested that by ledge-wise growth a plate originally nucleated at a certain region of the NbC–austenite interface gradually encircles the NbC particle, as is shown schematically in Fig. 9 (a–d). The edges of the plates have been observed to have different $\{111\}$ facets. Such variations in the plate geometry, a few examples of which have been shown in Fig. 7 (a–h) are associated with growth "diversions" caused by the presence of arrays of fine NbC particles precipitated on dislocations or in association with stacking faults. Possibly "superledges" nucleate at these impingement sites and further growth of the plates by the movement of these superledges gives rise to facets of different $\{111\}$ planes along the plate edges.

4. Conclusions

1. $M_{23}C_6$ precipitated around undissolved NbC particles nucleates at a site on the NbC–austenite interface that has an atomic stacking sequence close to that of a $\{111\}$ austenite plane. The precipitate nucleates with a low energy interface with the austenite.

2. The precipitate grows with planar edges by the formation and migration of ledges, and gradually encircles the undissolved particle at whose surface it has nucleated.

3. The ledge-wise growth of the precipitates produces a specific unique morphology, characteristic of the precipitating site, which is influenced by the presence of local strain energy/micro stress in the austenite lattice around the undissolved particles. The local stress fields developed during quenching due to the thermal contraction mismatch between NbC and austenite.

4. Different {111} facets develop at the precipitate edges due to growth diversions at the sites of impingement of the growing precipitate with the existing fine NbC precipitates and the nucleation of superledges at these sites.

References

1. J. M. SILCOCK, *JISI* **201** (1963) 409.
2. J. S. T. VAN ASWEGAN, R. W. K. HONEYCOMBE and D. H. WARRINGTON, *Acta Metall.* **12** (1964) 1.
3. J. M. SILCOCK and W. J. TUNSTALL, *Phil. Mag.* **10** (1964) 361.
4. F. H. FROES, R. W. K. HONEYCOMBE and D. H. WARRINGTON, *Acta Metall.* **15** (1967) 157.
5. M. C. CHATURVEDI, R. W. K. HONEYCOMBE and D. H. WARRINGTON, *JISI* **206** (1968) 1146.
6. *Idem*, *ibid.* **206** (1968) 1236.
7. J. M. SILCOCK and A. W. DENHAM, "The mechanism of phase transformations in crystalline solids", Institute of Metals Monograph No. 33. (Institute of Metals, London, 1969) p. 59.
8. J. P. SILCOCK, K. W. SIDDING and T. K. FRY, *Metal Sci. J.* **4** (1970) 29.
9. J. P. SHEPHERD, *ibid.* **3** (1969) 229.
10. N. TERAO and B. SASMAL, *Jpn. Inst. Metals* **22** (1981) 379.
11. B. HATTERSLEY and M. H. LEWIS, *Phil. Mag.* **10** (1964) 1075.
12. M. H. LEWIS and B. HATTERSLEY, *Acta Metall.* **13** (1965) 1159.
13. V. E. WOLFF, *Trans. MS-AIME* **236** (1966) 19.
14. L. K. SINGHAL and J. W. MARTIN, *Acta Metall.* **15** (1967) 1603.
15. F. R. BECKITT and B. R. CLARK, *ibid.* **15** (1967) 113.
16. L. K. SINGHAL and J. W. MARTIN, *Trans. MS-AIME* **242** (1968) 814.
17. *Idem. Acta Metall.* **16** (1968) 1159.
18. F. G. WILSON, *JISI* **209** (1971) 126.
19. N. TERAO and B. SASMAL, *Metallography* **13** (1980) 117.
20. *Idem. C.R. Acad. Sci.* (*Paris*) **287C** (1978) 487.
21. N. TERAO, *Jpn. J. Appl. Phys.* **3** (1964) 104.
22. H. GLEITER, *Acta Metall.* **17** (1969) 1421.
23. H. GLEITER and B. CHALMERS, *Prog. Mater. Sci.* **16** (1972) 77.
24. P. I. FILIMONOV, *Phys. Metals Metallog.* **18** (1964) 104.
25. B. SASMAL, PhD thesis. Indian Institute of Technology, Kharagpur, India, (1981).
26. J. P. ADAMSON and J. W. MARTIN, *Acta Metall.* **19** (1971) 1015.
27. H. I. AARONSON, "Decomposition of austenite by Diffusional Processes," (Interscience, New York, 1962) p. 387.
28. H. I. AARONSON, C. LAIRD and K. R. KINSMAN, "Phase transformations", (ASM, Metalo Park, 1970) p. 313.
29. A. MATSUZAKI, H. K. D. H. BHADESHIA and H. HARADA, in Proceedings of G. R. Speich Symposium, Montreal, 1992 (Iron and Steel Society, AIME, Warrendale, PA., 1992) p. 47.
30. J. W. STEWART, R. C. THOMSON and H. K. D. H. BHADESHIA, *J. Mater. Sci.* **29** (1994) 6079.
31. C. LAIRD and H. I. AARONSON, *Acta Metall.* **17** (1969) 505.
32. G. C. WEATHERLY, *ibid.* **19** (1971) 181.

Received 19 April 1996
and accepted 21 March 1997